isvr Institute of Sound and Vibration Research

Model for the Control of the Flow-Induced Noise Transmitted through a Stiffened Tensioned Double-Panel

C. Maury, P. Gardonio and S.J. Elliott

ISVR Technical Report No 300

June 2003

University of Southampton

SCIENTIFIC PUBLICATIONS BY THE ISVR

Technical Reports are published to promote timely dissemination of research results by ISVR personnel. This medium permits more detailed presentation than is usually acceptable for scientific journals. Responsibility for both the content and any opinions expressed rests entirely with the author(s).

Technical Memoranda are produced to enable the early or preliminary release of information by ISVR personnel where such release is deemed to the appropriate. Information contained in these memoranda may be incomplete, or form part of a continuing programme; this should be borne in mind when using or quoting from these documents.

Contract Reports are produced to record the results of scientific work carried out for sponsors, under contract. The ISVR treats these reports as confidential to sponsors and does not make them available for general circulation. Individual sponsors may, however, authorize subsequent release of the material.

UNIVERSITY OF SOUTHAMPTON

INSTITUTE OF SOUND AND VIBRATION RESEARCH

SIGNAL PROCESSING AND CONTROL GROUP

Model for the Control of the Flow-Induced Noise Transmitted through a Stiffened Tensioned Double-Panel

by

C. Maury, P. Gardonio and S. J. Elliott

ISVR Technical Report No 300

June 2003

Authorised for issue by
Prof S. J. Elliott
Group Chairman

Model for the Control of the Flow-Induced Noise Transmitted through a Stiffened Tensioned Double-Panel

CONTENTS

List of Figures

Figure 10. *The sound power radiated inward by an aircraft sidewall excited by a TBL when controlling the structural modes of the trim panel; thick solid line: before control; faint solid line: after cancellation of the first structural mode of the trim panel; dashed line: after cancellation of its two first structural modes; dotted line: after cancellation of its three first structural modes.*

Figure 11. *The sound power radiated inward by an aircraft sidewall excited by a TBL when controlling the cavity modes; thick solid line: before control; faint solid line: after cancellation of the first cavity mode; dashed line: after cancellation of its two first cavity modes; dotted line: after cancellation of its three first cavity modes.*

Figure A.1. *Transformation of the integration contour.*

ABSTRACT

The first objective of this report is to describe an extension of the analytical models already developed by the authors to predict, above 500 Hz, the Turbulent Boundary Layer-induced noise transmitted through aircraft panels (single and double panel models) towards the low-frequency range by considering TBL-excited tensioned and stiffened double-panel systems. A modal formulation coupled to a transfer matrix procedure has been developed and the analytical model is detailed in Section 2. Parametric studies including comparisons between different models of aircraft fuselage panels are analysed in Section 3.

The second objective of this study is to determine the best possible noise levels reduction that can be achieved using idealised feedback control of the boundary layer noise transmitted through the tensioned and stiffened double-panel partition. These results are discussed in Section 4.

One important conclusion of this study is that the prediction of the sound power inwardly radiated by an aircraft panel excited by a TBL should account for the dynamics of discretely stiffened skin panels since significant differences can be observed if the elastic stringers are replaced by simple-support boundary conditions.

However, accounting for the stiffening effect of stringers on the skin panel does not modify drastically the conclusions previously reached concerning the performance of active feedback control of the boundary layer induced noise for the double-panel model with rigid reinforcements: it is the strategy based on the active suppression of the skin panel structural modes that is the most efficient in terms of the broadband attenuation of the total sound power inwardly radiated.

1. INTRODUCTION

Acoustic comfort within the cabin of many commercial high-speed jet aircraft has lately become a subject of major concern. As aircraft propulsion and turbomachinery noise emissions are being further reduced, flow-induced noise has become more and more apparent. Moreover, the use of light composite structures for aircraft fuselage leads to an increase of the interior noise levels and thus justifies the need to develop innovative approaches for further noise reduction inside aircraft cabins. One can typically distinguish between two transfer paths for sound transmission into the cabin of aircraft structures: the structure-borne and the airborne sound transmission paths [1,2]. The former includes the propagation of the engines vibrations through the wing structure to the fuselage that then radiates sound into the cabin. The latter mainly gathers the acoustic excitation of the fuselage by the engine noise, the sound radiated within the cabin by the operation of air-conditioning systems and the flow-induced noise due to turbulent wall-pressure fluctuations imparted over the fuselage.

Under typical cruise conditions, the Turbulent Boundary Layer (TBL) noise contributes significantly to the interior noise with respect to other noise sources like jet engine noise or the noise due to air-conditioning systems. Experimental data obtained by Boeing [3, 4] have shown that the flow-induced noise efficiently excites aircraft fuselage structures over a broad frequency range up to 2 kHz. Aircraft sidewalls usually consist of stiffened double-partitions containing an insulating material. The damping treatments (which also provide heat insulation) are known to have a significant effect on reducing cabin noise levels in the high frequency range (typically greater than 500 Hz), but very little attenuation can be achieved in the low-frequency range [1]. It is therefore of interest to investigate the physical performance limitations of active control systems in order to reduce the levels of boundary layer noise transmitted through aircraft sidewalls in the low-frequency domain. It is the final objective of this study to assess the best possible levels of reduction that can be achieved for the boundary layer noise transmission when idealised feedback control systems are considered. This first requires the development of a simplified, but representative model to describe the response, in the low-frequency domain, of aircraft sidewalls excited by a TBL. Indeed, it is deemed that any successful technique for active flow-induced noise control will certainly arise from a deeper understanding concerning the physics of the vibro-acoustic phenomena involved and these latter should be captured through an efficient design and analysis tool.

Aircraft fuselage shells typically consist of a network of circumferential frames and longitudinal stringers covered by a thin aluminium skin. The interior part of the skin is in contact with insulation bags that are inwardly covered with composite trim panels. The skin panel is assumed to be excited by a fully-developed turbulent airflow. In-flight measurements taken by Bhat [3] and Wilby *et al.* [4] on a commercial aircraft have shown that, at high subsonic Mach numbers and for frequencies above about 500 Hz, the turbulent wall-pressure fluctuations excite the fuselage in such a way that the structural skin response is only correlated over a single fuselage panel, defined as the area between two neighbouring frames and stringers. Thus, within this frequency range, the vibrations between adjacent skin panels are largely incoherent and models describing boundary layer noise transmission through individually vibrating skin panels (eventually trimmed) are representative in the prediction of the flow-induced noise radiated into aircraft cabin, only above 500 Hz. However, in order to examine the performance of active control systems for the reduction of interior noise due to TBL, a model valid in the low-frequency domain is needed and a suitable candidate should

consider an array of flexible skin panels accounting for the effect of elastic stiffeners. Hence, for sake of completeness, the authors have developed three models for the prediction and control of the boundary layer noise transmitted through aircraft sidewalls: a single panel model [5, 6, 7], a double-panel model [8] and a stiffened double-panel model. It is the detailed analysis of the latter model that will be presented in this report. In the following subsection, a schematic (and necessarily incomplete) review of different classes of simplified models that can be found in the literature for the vibro-acoustic response of TBL-excited aircraft sidewalls is attempted.

1.1 A brief review of different models predicting TBL-induced noise

Most of the studies on the TBL-induced noise have considered the individual panels model since it retains the essential features of the problem (at least above 500 Hz) while providing an analytical formulation for the quantities of interest. Early simulations using a modal formulation have been made by Crocker [9] in order to compare the structural response of aircraft panels either excited by a TBL or by an acoustic diffuse field. The aim was to use equivalent reverberant acoustic fields that would produce the same overall response as the one due to a TBL. If successful, this technique would avoid the need to perform expensive and delicate in-flight or wind-tunnel measurements in order to know the response of TBL-excited fuselage structures. Numerical as well as experimental data have shown that the sound power radiated by an aircraft panel is about 10 to 20 dB higher for an acoustic diffuse field excitation than for a TBL excitation. Further studies have demonstrated that the difference in the resonant contribution scales on the squared ratio between the acoustic wavelength and the TBL correlation lengths evaluated at each resonant frequency [10]. Practically, since the difference between the two responses is not uniform over a broad frequency range, it seems that the simulation of boundary layer noise with reverberant noise is of limited use.

A seminal study using the single panel model was made by Davies [11] in order to derive the statistical properties of the sound power radiated by TBL-excited panels starting from a modal representation of the system response. In this work, conditions have been initially proposed such that the modal cross-coupling excitation terms can be neglected. This provides a considerable simplification in the problem formulation, thus more amenable to a closed form solution. Several other investigations, based on a modal approach, have considered a formulation for the excitation and sound radiation mechanisms either in the space-time domain [12], in the space-frequency domain [13, 14] or in the wavenumber-frequency domain [15, 6], in order to predict the vibro-acoustic response of TBL-excited panels. The latter formulation presents the advantage to account for a large number of models for the fluctuating boundary layer pressures defined by their wavenumber-frequency spectrum. Recent studies have been performed that determine which model of the wall-pressure fluctuations is more appropriate with respect to the frequency range or the Mach number of interest [16, 17]. A wavenumber-frequency analysis also allows a direct physical interpretation of the spectral distribution of the system response, especially in terms of filtering of the excitation spectrum by the *sensitivity* function of the system [7].

Models predicting the high-frequency response of TBL-excited panels have also been developed using approaches based either on the Statistical Energy Analysis (SEA) [18, 19] or on the Energy Flow Analysis (EFA) [20]. Both methods consider space and frequency averaged quantities of vibratory and acoustic energy. The SEA assumes a large modal density of the structure over small frequency bands. These modes are known as *resonant* modes and

have been shown to significantly contribute to the vibratory energy of TBL-excited panels with respect to the *non-resonant* modes whose frequencies lies outside the band of interest [21]. Recent comparisons between the vibratory response calculated with the program AutoSEA2 and experimental data obtained on Boeing flight tests [4] have shown a good agreement for frequencies above 1 kHz [22]. However, it is likely that, in the SEA method, the contributions of non-resonant modes with high radiation efficiencies may be of importance with respect to the contribution of resonant modes in order to predict the levels of acoustic energy radiated by the TBL-excited panel. This point is still questionable. As an alternative, the EFA method has been recently proposed to predict the spatial variation of the spatially and frequency averaged energy density of a structure as a solution of the energy flow equation with the input power density due to a random excitation as a forcing term. The energy density is sought as a series of the panels modes with the coefficients describing the spatial match between the input power density of the excitation and the spatial variations of each mode. This method has been successfully applied to predict the vibroacoustic response of a panel excited by a separated-reattached flow [20]. Unlike in the SEA approach, the EFA method can also account for complex structural-acoustic systems whose natural modes can be calculated with a Finite Element method. However, as expected, both methods have shown a poor agreement with results obtained in the low-frequency domain from classical modal formulations [20, 22].

Analytical and semi-analytical models accounting both for the structural complexity of aircraft sidewalls and their excitation by a random field are much more limited. A first group of investigations in this field concerns the use of a "wave-like" approach. One of the first analysis has been made by Mead *et al.* to describe the response of periodically stiffened beams to boundary layer excitation by means of a space harmonic analysis using a flexural wave propagation approach [23, 24]. It has been shown that the maximum response of the system is determined by the wavenumber components of the random excitation that coincide with those of free propagating waves in the structure. This approach has proved to be computationally efficient with respect to normal mode analysis whatever the magnitude of the structural damping. More recently, an attempt has been made to couple the "wave-approach" with a Finite Element model. It has resulted in a new methodology called the Spectral Finite Element Method (SFEM), formulated in the wavenumber-frequency domain. It has been successfully applied to the prediction of the structural response of TBL-excited panels [25]. In general, the "wave-approach" is more applicable to study acoustic and vibration transmission through waveguide-like structures whereas Finite Element formulations account more readily for composite built-up structures like stiffened double-panel systems.

In parallel, other semi-analytical methods have been developed that are either based on a modal expansion of the solution [26, 27, 28, 29, 30, 31, 32] or on analytical approximations that are sufficient to estimate the frequency-averaged response characteristics of the TBL-excited structure [33, 34, 35]. Initially, a full theoretical formulation has been obtained by Mkhitarov [26] to describe the sound radiated by a fluid-loaded stiffened panel driven by boundary layer pressure fluctuations. In this work, the natural modes of the stiffened panel are defined by the set of coefficients of their Fourier cosine series. This leads to a modal representation of the solution that seems hardly tractable in view of a simplified model. Transfer matrix techniques provide an alternative that enables to keep a closed-form expression for the natural modes of discretely stiffened structures [27, 28]. This procedure has been used in parallel with modal decomposition techniques to predict boundary-layer noise transmission through finite stiffened panels into rectangular enclosures [29, 30, 31] and

boundary-layer noise transmission through discretely stiffened curved panels into semi-cylindrical enclosures [32]. These semi-analytical studies have shown how geometrical and mechanical parameters as well as damping and acoustic absorption materials can affect the levels of boundary-layer noise transmitted in the low-frequency domain. Lately, a simplified estimate has been proposed by Rumerman [33, 34, 35] for the broadband acoustic power due to a rib-stiffened panel driven by TBL pressure fluctuations, assuming that the ribs radiate independently. This assumption is only valid for frequencies at which the acoustic wavelength is smaller than about four times the rib spacing, i.e. above 2 kHz for typical aircraft panels. The simplified model derived by Rumerman is thus mostly applicable for predictions in the high frequency domain.

The models discussed above provide valuable and complementary tools to analyse the response of TBL-excited composed structures over a broad frequency range. However, given the need for further interior noise reduction, it is imperative to determine numerically and experimentally to which extent active control systems can perform in the low-frequency domain.

1.2 Flow-induced noise control techniques

Very few results have been obtained up to now for the active control of the boundary layer-induced noise (or more generally to actively control broadband random disturbances generated either by boundary layer flow or by jet noise). Most of the previous studies have concentrated on the reduction of harmonic interior noise and vibrations. Their efficiency has been demonstrated to reduce the multitonal noise generated by propellers and turbomachinery [1, 2]. For instance, Tunable Vibration Absorbers (TVA) have been designed to reduce vibration levels, and therefore cabin interior noise at discrete frequencies in the low-frequency domain [36]. However, an inherent tradeoff has been observed between the control performance and the bandwidth over which it shows efficiency. We note that TVA devices belong to ***passive*** noise control techniques since they do not require any power input.

Active noise control techniques have also been investigated and previous work has mainly considered three control arrangements: active noise control (ANC) in the receiving enclosure [37]; active structural acoustic control (ASAC) using vibrational control sources on the radiating panel [38]; and cavity control by means of acoustic sources inserted in the gap within the double-partition in order to block the airborne transmission path [39]. As confirmed by numerical predictions and experiments, the ANC and cavity control strategies are mostly effective in the very low frequency domain with the cavity control approach being more effective in achieving global reduction of the noise levels. On the other hand, the ASAC approach provides significant noise reduction over a broader frequency range assuming plane waves excitation of the double-panel system [40, 41].

In practice, ANC systems are now in use in propeller aircraft and can provide interior noise reduction of up to 25 dB according to the seat location [37]. These systems use microphone and accelerometer sensors, loudspeakers actuators and DSP controllers. They are mostly implemented using a ***feed-forward*** architecture since a reference signal that is strongly correlated with the harmonic disturbance is readily available. Moreover, the periodicity of the disturbance can significantly reduce the processing burden on the controller. On the other hand, it appears that ***feedback*** devices are more adapted to the active control of TBL-induced noise than feed-forward architectures. Indeed, the random nature of the airflow noise, the

subsequent difficulty to obtain a time-advanced reference signal that is highly correlated to the random disturbance, the complexity of the transmission path through the fuselage structure and the weak correlation that results between the signal at the reference sensors and at the error sensors makes difficult any practical implementation of feed-forward control of TBL-induced noise. This strategy would then require a prohibitive number of sensors and actuators in order to achieve significant reductions of the boundary layer noise transmitted.

It is worth noting that, in most applications, active control systems make use of a centralized controller which is connected to a large number of distributed sensors and actuators [42]. This configuration often presents the drawback to be costly, to add weight and to present a limited reliability. As an alternative, a decentralized control system --- where sensors, actuators and controllers are localized --- would enable decreasing costs, integration in small self-contained units (using MEMS technology) and better reliability [43]. This architecture may be a future practical solution to implement active control of TBL-induced interior noise since, in order to be efficient, many independent ***feedback*** control units need to be applied over a large area of the aircraft's interior fuselage surface [44]. Promising results have already been obtained in this direction. In particular, the feasibility of reducing broadband radiation from multiple panels excited by a TBL has recently been demonstrated by Gibbs *et al.* [45] using simultaneous independent feedback control of each panel. The fuselage portion consisted of six panels separated by stiffeners and a single-input/single-output configuration was used for each control unit. The results have shown reductions of up to 7.5 dB for the radiated sound power integrated over the bandwidth 150-800 Hz at a flow speed of Mach 0.125. As observed by Gibbs *et al.*, the performance of the control system may have been limited by the cross-coupling effect between the panels. We note that the simplified model presented in this report accounts for this cross-coupling effect and its analysis may be useful to examine the performance limitations of idealised feedback control systems in order to actively reduce the TBL-induced sound radiated from multiple aircraft panels.

In parallel to progresses in control architectures and given the need to achieve subsequent reductions in interior noise levels during the next decades, research will also be needed in material optimisation such as the design of optimally shaped piezoceramic (PZT) actuators [46] or the combination of active and passive materials, such as acoustic foam to damp higher frequencies and PZT transducers to actively control lower frequencies [47]. For instance, boundary layer noise reduction of up to 6 dB(A) integrated from 400-1000 Hz at flow speeds of Mach 0.2 have already been achieved experimentally by means of active/passive foam elements mounted on an aircraft panel and used in conjunction with a feedforward control approach [47]. However, such a multi-input/multi-output scheme seems difficult to implement in practice for a typical aircraft fuselage which consists of several hundreds of such panels. A hierarchical control approach which can handle very high order control systems may then prove useful in this configuration [48].

Several analytical studies have considered feedback control of the TBL-induced sound and vibration, but the research effort in this area is still very sparse. An optimal control approach has been studied analytically by Thomas *et al.* [49]. In this work, promising noise reductions of 25 dB at the first panel resonance have been predicted using feedback control of the TBL-induced structural radiation and assuming that a full state of the system (TBL excitation, plate response and radiation) is known at all times for the design of an optimal state feedback controller. Although this type of control has already shown good results for actively controlling the vibrations of a panel flush-mounted in the test section of an anechoic wind-

tunnel [50], the computational burden of this approach makes difficult any practical implementation of this system in an aircraft. As an alternative, a frequency domain controller, robust to plant variations and model uncertainties, has been designed by loop shaping of the controller transfer function, thus limiting the approach to the low-frequency domain [51].

Physical limitations of actively controlling the sound power inwardly radiated by TBL-excited aircraft panels (single and double panel model) have been discussed by the authors [5, 8] and successful comparisons on the single panel case with recent experimental results [52, 53] have shown the validity of the model developed. It is the first objective of this report to describe an extension of these analytical models in order to predict the vibro-acoustic response of TBL-excited tensioned and stiffened double-panel systems. A modal formulation coupled to a transfer matrix procedure has been developed and the model is detailed in Section 2. Parametric studies including models comparisons are analysed in Section 3. The second goal of this study is to determine the best possible noise levels reduction that can be achieved using idealised feedback control of the boundary layer noise transmitted through the double-panel partition. These results are discussed in Section 4 and the main conclusions of this study are presented in Section 5.

2. RESPONSE OF A STIFFENED TENSIONED DOUBLE-PANEL TO A TURBULENT BOUNDARY LAYER EXCITATION

2.1 The stiffened double-panel model

Aircraft fuselage shells consist of a network of circumferential frames and longitudinal stringers covered by a thin aluminium skin. The interior part of the shell is in contact with insulation bags filled with a fiberglass treatment and is inwardly covered with plastic trim panels. Figure 1 shows a sketch of an aircraft sidewall cross-section the outer part of which is made of an array of panels reinforced by elastic stiffeners. The skin panel is excited by a fully-developed turbulent airflow.

In-flight measurements have shown that, at high subsonic Mach numbers and for frequencies above 500 Hz, the boundary layer correlation lengths are significantly smaller than the dimensions of typical fuselage panels and so, the vibrations between adjacent panels are largely incoherent [4]. Thus, models describing noise transmission through individually vibrating skin panels (eventually trimmed) are representative in the prediction of boundary layer induced noise in aircraft at high frequencies [8, 15, 54]. However, in order to examine the performance of active control systems for flow-induced noise, a model valid at low frequencies is required and a suitable candidate should consider an array of flexible panels accounting for the effect of elastic stiffeners, as in the system shown in Figure 1.

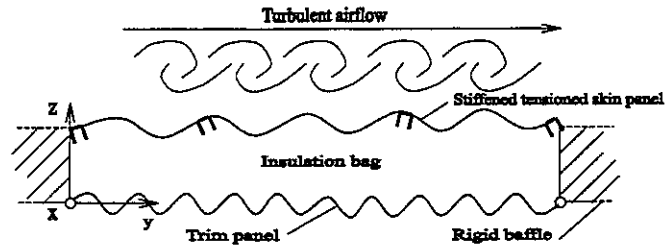

Figure 1. The stiffened double-panel model.

The skin panel in this paper is modelled by three aluminium flat plates connected by stiffeners and in contact with frames and stringers along the edges respectively in the streamwise and in the spanwise directions. The stiffeners are assumed to have the same mechanical characteristics as the skin panel [4]. Because of the cabin pressurisation effect, the skin panel is stressed by tension forces and the influence of panel curvature on the interior sound level can be neglected with respect to the tensioning effect. The trim panel is modelled by a simply-supported flat composite plate and the cavity is assumed to contain an insulation bag filled with a fiberglass material. The physical constants for typical aircraft sidewalls are listed in Table 1.

Airflow	
Free-stream velocity	$U_\infty = 225\,\text{m/s}$
r.m.s. wall pressure	72.6 Pa
External air density	$\rho_e = 0.53\,\text{kg/m}^3$
External sound speed	$c_e = 310\,\text{m/s}$
Skin panel	
Dimensions	$l_{s,x} = 0.20\,\text{m}, l_{s,y} = 3\times 0.17\,\text{m}$
Thickness	$h_s = 0.0015\,\text{m}$
Mass density	$\rho_s = 2700\,\text{kg/m}^3$
Young's modulus	$E_s = 7.1\times 10^{10}\,\text{Pa}$
Poisson ratio	$\upsilon_s = 0.33$
Damping ratio	$\xi_s = 0.01$
Streamwise tension	$N_y = 29.3\times 10^3\,\text{N/m}$
Spanwise tension	$N_x = 62.1\times 10^3\,\text{N/m}$
Stringers	
Cross-sectional area	$A = 1.48\times 10^{-4}\,\text{m}^2$
Warping constant	$C_w = 4.42\times 10^{-12}\,\text{m}^6$
St.Venan torsion constant	$C_t = 9.42\times 10^{-11}\,\text{m}^4$
Moments of inertia	$I_{zz} = 3.45\times 10^{-8}\,\text{m}^4,\ I_{yy} = 5.07\times 10^{-8}\,\text{m}^4$
	$I_{zy} = 0,\ J_S = 1.057\times 10^{-7}\,\text{m}^4$
Shear center distances	$c_z = 0.02\,\text{m},\ c_y = 0,\ s_z = 0.002\,\text{m}$
Shear elastic modtulus	$g_S = 2.78\times 10^{10}\,\text{Pa}$
Trim panel	
Dimensions	$l_{t,x} = 0.20\,\text{m}, l_{t,y} = 0.51\,\text{m}$
Thickness	$h_t = 0.004\,\text{m}$
Mass density	$\rho_t = 255\,\text{kg/m}^3$
Young's modulus	$E_t = 1.5\times 10^9\,\text{Pa}$
Poisson ratio	$\upsilon_t = 0.3$
Damping ratio	$\xi_t = 0.05$
Dissipative material (fiberglass)	
Thickness	$d = 0.07\,\text{m}$
Flow resistivity	$\sigma = 12000\,\text{N m}^{-4}\text{s}$
Equivalent fluid constants	$c_1 = 0.070, c_2 = -0.632, c_3 = 0.107, c_4 = -0.632$
Model of [14]	$c_5 = 0.160, c_6 = -0.618, c_7 = 0.109, c_8 = -0.618$

Table 1. *Physical constants for typical aircraft sidewalls.*

2.2 Modal analysis

A modal formulation is used to predict the vibro-acoustic response of the stiffened panel-cavity-panel system to a TBL excitation since this leads to an analytical solution that enables parametric studies to be performed at a low computational cost. In this method, the deflections, w_s and w_t, of the skin panel and the trim panel are expanded as a finite series of N_s and N_t orthogonal functions corresponding to the structural modes, $\psi_{s,m}$ and $\psi_{t,m}$, of respectively, the stiffened tensioned skin panel and the trim panel. The cavity pressure field, p_a, is sought as a series of N_a orthogonal acoustic modes F_n of the rigid wall cavity, so that:

$$w_{\{s,t\}}(x,y;t)=\sum_{n=1}^{N_{\{s,t\}}} q_{\{s,t\},n}(t)\psi_{\{s,t\},n}(x,y)=\Psi_{\{s,t\}}^{\mathrm{T}}\mathbf{q}_{\{s,t\}}, \tag{1}$$

$$p_a(x,y,z;t)=\sum_{p=0}^{N_a} a_p(t)F_p(x,y,z)=\mathbf{F}^{\mathrm{T}}\mathbf{a}, \tag{2}$$

where $\Psi_{\{s,t\}}$ and $\mathbf{F}$ are respectively the $N_{\{s,t\}}$-length vectors of the panels structural mode shapes and the N_a-length vector of the cavity mode shapes. $\mathbf{q}_{\{s,t\}}$ and $\mathbf{a}$ are, respectively, the vector of complex structural modes amplitudes and the vector of complex cavity modes amplitudes. The structural modes of the υ-th span of the stiffened and tensioned skin panel have the form:

$$\psi_{s,n}(x,y)=\sin\left(\frac{n\pi x}{b}\right)Y_{n(m)}^{(\nu)}(y-(\nu-1)\tilde{a}),\quad \tilde{a}=\frac{a}{N},$$
$$x\in[0,b],\quad y\in[(\nu-1)\tilde{a},\nu\tilde{a}],\quad \nu=1,\ldots,N, \tag{3}$$

where N is the number of spans of the stiffened skin panel. In particular, the normal modes of the υ-th span corresponding to the y direction are sought as:

$$Y_{n(m)}^{(\nu)}(y)=\sum_{i=1}^{4}\kappa_{in(m)}^{(\nu)}\varphi_i\left(k_{in(m)}y\right),\quad y=0,\ldots,\tilde{a}, \tag{4}$$

with the normal wavenumbers and eigenfunctions summarized in the following table:

i	**1**	**2**	**3**	**4**
φ_i	sin	cos	sinh	cosh
$k_{in(m)}$	$\sigma_{n(m)}^{-}$	$\sigma_{n(m)}^{-}$	$\sigma_{n(m)}^{+}$	$\sigma_{n(m)}^{+}$

and

$$\sigma_{n(m)}^{\pm}=\left[\left(\frac{\rho_s h_s\omega_{n(m)}^2}{D_s}+\frac{N_y^2}{4D_s^2}+\left(\frac{n\pi}{b}\right)^2\left(N_y-N_x\right)\right)^{1/2}\pm\left(\frac{n\pi}{b}\right)^2\pm\frac{N_y}{2D_s}\right]^{1/2}, \tag{5}$$

where $D_s=E_s h_s^3/12(1-\upsilon_s^2)$ is the flexural rigidity of the skin panel; N_x and N_y are respectively the lateral and longitudinal tensions of the skin panel. Eq. (5) represents the

characteristic roots of a bi-quadratic differential equation obtained after substituting, for each $n(m)$, the modal form $\varphi_i(k_{in(m)}y)$ into the plate-bending equation of motion for the tensioned skin panel. In Eq. (4), $\omega_{n(m)}$ and $\kappa_{i,n(m)}^{(v)}$ (i=1,..,4, v=1,...,N) are respectively the natural frequencies of the skin panel and proportionality factors. These latter quantities are determined by using a transfer matrix method where boundary-contact conditions are satisfied across each span for the deflection, slope, moment and shear of the skin panel [27, 28].

Following a Galerkin procedure, one can substitute Eqs. (1) and (2) into the governing equations of motion for the panels and the acoustic cavity. Using the orthogonality properties of the mode shape functions, a set of $(N_s + N_t + N_a + 1)$ coupled algebraic equations is then obtained. It reads:

$$M_{i,n}\left[\ddot{q}_{i,n} + 2\xi_{i,n}\omega_{i,n}\dot{q}_{i,n} + \omega_{i,n}^2 q_{i,n}\right] = -\rho_a A_i \sum_{p=0}^{N_a} \dot{a}_p L_{i,pn} + Q_{s,n}^e, \quad i = \{s,t\}, \tag{6}$$

$$V_a M_{a,p}\left[\ddot{a}_p + \left(c_a\omega_{a,p}/c_0\right)^2 a_p\right] = c_a^2 A_s \sum_{n=1}^{N_s} L_{s,pn}\dot{q}_{s,n} + c_a^2 A_t \sum_{n=1}^{N_t} L_{t,pn}\dot{q}_{t,n}, \tag{7}$$

where $M_{i,n}, M_{a,p}$ are the generalized masses and $\omega_{i,n}, \omega_{a,p}$ are the natural frequencies corresponding to the n-th panels mode and to the p-th cavity mode. For the stiffened skin panel, the generalized mass is given by:

$$M_{s,n} = \rho_s h_s \int_{A_s} \psi_{s,n}^2 dA_s + \sum_{j=1}^{4} \rho_s A \int_0^{l_{s,x}} \psi_{s,n}^2\left(x,(j-1)l_{s,y}\right)dx. \tag{8}$$

In Eq. (6), $\xi_{i,n}$ is the damping ratio of the n-th structural mode of each panel. $A_{\{s,t\}}$ and V are the panels surface and the cavity volume respectively. $\{Q_{s,n}^e\}$ are the generalized forces corresponding to the external pressures imparted on the skin panel. c_a and ρ_a are respectively the sound speed and the density of the fluid within the cavity. When the cavity contains a fiberglass material, we use complex equivalent fluid parameters to model its acoustic properties. They are given by the model of Delany and Bazley [55]. The coefficients $L_{\{s,t\}pn}$ describe the coupling between the n-th panels mode and the p-th cavity mode. Using a matrix formulation, Eqs. (6) and (7) can be written as follows:

$$\mathbf{M}\ddot{\mathbf{X}} + \mathbf{C}\dot{\mathbf{X}} + \mathbf{S}\mathbf{X} = \mathbf{Q}^e, \tag{9}$$

where $\mathbf{M}$, $\mathbf{C}$ and $\mathbf{S}$ are respectively the mass matrix, the sum of the coupling and damping matrices and the stiffness matrix. $\mathbf{X}$ is the vector of the modal amplitudes and $\mathbf{Q}^e$ is the vector of generalized forces due to TBL pressure fluctuations over the panel.

Assuming that the statistics of the boundary layer wall-pressure fluctuations are stationary with respect to time and space variables, the spectral density $\Phi_e(r_x, r_y; \omega)$ of the fluctuating wall pressure field can be described as a product between an averaged autospectral density

function $\Phi_0(\omega)$ and a coherence function $C_{pp}(r_x, r_y; \omega)$ between two points which are a distance r_x apart in the spanwise direction and r_y apart in the streamwise direction, so that, when using a Corcos model of the TBL excitation, one obtains [56]:

$$\Phi_e(r_x, r_y; \omega) = \Phi_0(\omega) e^{-\omega r_x/\alpha_x U_c} e^{-\omega r_y/\alpha_y U_c} e^{i\omega r_y/U_c}, \tag{10}$$

It is assumed that the coherence function can be written in a separable form, as follows:

$$C_{pp}(r_x, r_y; \omega) = C_{pp}^{sp}(r_x; \omega) C_{pp}^{st}(r_y; \omega) = e^{-K_x|r_x|} e^{-K_y|r_y|} e^{ik_c r_y}, \tag{11}$$

where the wavenumbers are defined as:

$$\begin{cases} r_y = y - y', \quad K_y = \dfrac{\omega}{\alpha_y U_c}, \quad k_c = \dfrac{\omega}{U_c}, \\ r_x = x - x', \quad K_x = \dfrac{\omega}{\alpha_x U_c}. \end{cases} \tag{12}$$

$U_c \approx 0.7 U_\infty$ is the convection velocity, U_∞ is the free-stream velocity and the empirical coefficients α_x and α_y are usually taken to be 1.2 and 8.

We are primarily interested in the prediction of the spectrum $\Phi_{W_r}(\omega)$ of the sound power inwardly radiated by the trim panel. It can be written as [8]:

$$\Phi_{W_r}(\omega) = \frac{\rho_0 c_0 \omega^2}{2} \mathrm{Tr}\left[\Phi_{q_t q_t} \Re[\mathbf{Z}]\right], \tag{13}$$

where $\Re[\mathbf{Z}]$ is the modal radiation resistance matrix. $\Phi_{q_t q_t}$ is the $(N_t \times N_t)$ spectral density (SD) matrix between the modal amplitudes of the trim panel deflection. It can be expressed in terms of the $(N_s \times N_s)$ CSD matrix Φ_{Q^e} between the generalized random forces of the excitation as follows:

$$\Phi_{q_t q_t} = \mathbf{L}^{-1} \begin{bmatrix} \Phi_{Q^e} & \mathbf{0} & \mathbf{0} \\ \mathbf{0} & \mathbf{0} & \mathbf{0} \\ \mathbf{0} & \mathbf{0} & \mathbf{0} \end{bmatrix} \left(\mathbf{L}^{-1}\right)^{\mathrm{H}}, \tag{14}$$

where $\mathbf{L} = -\omega^2 \mathbf{M} + i\omega \mathbf{C} + \mathbf{S}$ (see Eq.(9)).

2.3 Evaluation of the modal excitation terms

Analytical expressions have been derived for each element of Φ_{Q^e}, also called the modal joint acceptance functions. These functions describe how the structural modes of the stiffened

skin panel are coupled through the TBL excitation. It is worth noting that the models described in [29, 30, 31, 32] use a numerical evaluation of the elements of Φ_{Q^e}. This lengthy procedure represents the main computational burden of these methods. However, it is possible to derive a full analytical formulation of the solution, as shown in this section, thus dramatically reducing the numerical cost. Although this derivation does not present any qualitative difficulties, similar results have not been found by the authors in the literature already published on the subject.

Each element $J_{\substack{r=(m,n)\\ s=(p,q)}}$ of the CSD matrix Φ_{Q^e} can be written as a quadruple integral over the skin panel area that can be expressed in terms of the modal excitation functions $J^{(v)}_{\substack{mn\\ pq}}$ of each span, as follows:

$$\begin{aligned} J_{\substack{mn\\ pq}}(\omega) &= \iint_{\Sigma} \psi_{n(m)}(x,y) C_{pp}(r_x, r_y; \omega) \psi^*_{q(p)}(x',y') dx dy dx' dy' \\ &= \sum_{v=1}^{N} \sum_{v'=1}^{N} J^{(v)}_{\substack{mn\\ pq}}(\omega), \end{aligned} \tag{15}$$

where

$$J^{(v)}_{\substack{mn\\ pq}}(\omega) = \int_0^b \int_{(v-1)\bar{a}}^{v\bar{a}} \int_0^b \int_{(v-1)\bar{a}}^{v\bar{a}} \psi^{(v)}_{n(m)}(x,y) C_{pp}(x-x', y-y'; \omega) \psi^{(v)*}_{q(p)}(x',y') dx dy dx' dy'. \tag{16}$$

In Eq. (15) and in the subsequent expressions, the subscript s referring to the skin panel normal modes is omitted. The modal excitation function of the v-th span (Eq. (16)) can be factorised, according to (11), as the product of two double integrals defined respectively in the streamwise and in the spanwise directions. It reads:

$$J^{(v)}_{\substack{mn\\ pq}}(\omega) = J^{(v)}_{mp}(\omega) J_{nq}(\omega), \tag{17}$$

where $J^{(v)}_{mp}$ and J_{nq} take the form:

$$J^{(v)}_{mp}(\omega) = \int_0^{\bar{a}} \int_0^{\bar{a}} Y^{(v)}_{n(m)}(y) C^{st}_{pp}(y-y'; \omega) Y^{(v)*}_{q(p)}(y') dy dy', \tag{18}$$

$$J_{nq}(\omega) = \int_0^b \int_0^b \sin\left(\frac{n\pi x}{b}\right) C^{sp}_{pp}(x-x'; \omega) \sin\left(\frac{q\pi x'}{b}\right) dx dx'. \tag{19}$$

After substituting Eq. (4) into the integral (18), one obtains for the modal excitation term of the v-th span along the streamwise direction:

$$J^{(v)}_{mp}(\omega) = \sum_{i=1}^{4} \sum_{l=1}^{4} \chi^{n(m)q(p)}_{il} I_{il}\left(k_{in(m)}, k_{lq(p)}; \omega\right), \tag{20}$$

where

$$I_{il}\left(k_{in(m)},k_{lq(p)};\omega\right)=\int_0^{\tilde{a}}\int_0^{\tilde{a}}\varphi_i\left(k_{in(m)}y\right)C_{pp}^{st}\left(y-y';\omega\right)\varphi_l^*\left(k_{lq(p)}y'\right)dydy', \tag{21}$$

and with the following combination of the coefficients:

$$\chi_{il}^{n(m)q(p)}=\sum_{\nu=1}^{N}\sum_{\nu'=1}^{N}K_{in(m)}^{(\nu)}K_{lq(p)}^{(\nu')*}. \tag{22}$$

We note, from Eq. (19), that:

$$J_{nq}=I_{11}\left(\frac{n\pi}{b},\frac{q\pi}{b}\right)_{\substack{K_y=K_x\\ k_c=0\\ \tilde{a}=b}} \tag{23}$$

After performing some algebra on Eq. (21), the following connective relations are obtained:

$$\begin{cases} I_{13}\left(k_{2n(m)},k_{1q(p)}\right)=jI_{11}\left(k_{2n(m)},jk_{1q(p)}\right)\\ I_{31}\left(k_{1n(m)},k_{2q(p)}\right)=-jI_{11}\left(jk_{1n(m)},k_{2q(p)}\right)\\ I_{33}\left(k_{1n(m)},k_{1q(p)}\right)=I_{11}\left(jk_{1n(m)},jk_{1q(p)}\right)\end{cases}\quad\begin{cases} I_{42}\left(k_{1n(m)},k_{2q(p)}\right)=I_{22}\left(jk_{1n(m)},k_{2q(p)}\right)\\ I_{24}\left(k_{2n(m)},k_{1q(p)}\right)=I_{22}\left(k_{2n(m)},jk_{1q(p)}\right)\\ I_{44}\left(k_{1n(m)},k_{1q(p)}\right)=I_{22}\left(jk_{1n(m)},jk_{1q(p)}\right)\end{cases}$$

$$\begin{cases} I_{32}\left(k_{1n(m)},k_{2q(p)}\right)=-jI_{12}\left(jk_{1n(m)},k_{2q(p)}\right)\\ I_{14}\left(k_{2n(m)},k_{1q(p)}\right)=I_{12}\left(k_{2n(m)},jk_{1q(p)}\right)\\ I_{34}\left(k_{1n(m)},k_{1q(p)}\right)=-jI_{12}\left(jk_{1n(m)},jk_{1q(p)}\right)\end{cases}\quad\begin{cases} I_{23}\left(k_{2n(m)},k_{1q(p)}\right)=jI_{21}\left(k_{2n(m)},jk_{1q(p)}\right)\\ I_{41}\left(k_{1n(m)},k_{2q(p)}\right)=I_{21}\left(jk_{1n(m)},k_{2q(p)}\right)\\ I_{43}\left(k_{1n(m)},k_{1q(p)}\right)=jI_{21}\left(jk_{1n(m)},jk_{1q(p)}\right)\end{cases} \tag{24}$$

It can be observed that $I_{21}(\alpha,\beta)=I_{12}^*(\beta^*,\alpha^*)$ where α and β denote complex numbers. One shall then realize that, once I_{11}, I_{12} and I_{22} have been calculated, all the integrals that appear in (20) can be determined via the symmetries.

Introducing the generic notation:

$$I(\alpha,\beta)=\int_0^{\tilde{a}}\int_0^{\tilde{a}}e^{i(\alpha y+\beta y')}e^{-K_y|y-y'|}e^{ik_c(y-y')}dydy' \tag{25}$$

The following relations can then be readily obtained:

$$\begin{cases} I_{11}(\alpha,\beta)=\frac{1}{4}\left[I(\alpha,-\beta)+I(-\alpha,\beta)-I(\alpha,\beta)-I(-\alpha,-\beta)\right]\\ I_{12}(\alpha,\beta)=\frac{1}{4i}\left[I(\alpha,-\beta)-I(-\alpha,\beta)+I(\alpha,\beta)-I(-\alpha,-\beta)\right]\\ I_{22}(\alpha,\beta)=\frac{1}{4}\left[I(\alpha,-\beta)+I(-\alpha,\beta)+I(\alpha,\beta)+I(-\alpha,-\beta)\right]\end{cases} \tag{26}$$

The integral (25) can be evaluated analytically. The details are given in Appendix A. Two cases must be distinguished:

If $\alpha+\beta\neq 0$:

$$I(\alpha,\beta)=\frac{1}{i(\alpha+\beta)}\left\{e^{i(\alpha+\beta)}\left[F\left(-i(\beta-k_c)-K_y\right)+F\left(-i(\beta+k_c)-K_y\right)\right]\right. \\ \left.-\left[F\left(i(\alpha+k_c)-K_y\right)+F\left(i(\alpha-k_c)-K_y\right)\right]\right\}, \tag{27.a}$$

If $\alpha+\beta=0$:

$$I(\alpha,\beta)=\frac{2aK_y}{K_y^2+(k_c-\beta)^2}+2\Re\left[\frac{F\left(-i(\beta-k_c)-K_y\right)}{-i(\beta-k_c)-K_y}\right], \tag{27.b}$$

where: $F(z)=\dfrac{e^z-1}{z}$. From (27.a) and (27.b), substituted into Eqs. (26, 24, 23, 20, 17, 15), each element $J_{\substack{mn\\pq}}$ of the CSD matrix Φ_{Q^e} can then be calculated.

2.4 Resonances equation

The resonance frequencies and the corresponding resonance modes of the tensioned stiffened double-panel system are defined as the non-trivial solutions, in the frequency domain, of the homogeneous system of equations associated to Eq. (9), or resonances equation. By use of matrix notations, it can be formulated as a standard polynomial eigenequation:

$$\left(\lambda^2\mathbf{M}+\lambda\mathbf{C}+\mathbf{S}\right)\mathbf{X}=\mathbf{0}, \tag{28}$$

where the imaginary part $\Im[\lambda]$ of each eigenvalue λ is related to the real part $\Re[f]$ of a resonance frequency of the system via $\Re[f]=\Im[\lambda]/2\pi$ and the real part corresponds to the damping of the mode (or the modal decay time) via $\Im[f]=-\Re[\lambda]/2\pi$. The components of the eigenvector or resonance mode, $\mathbf{X}$, can be used to describe how the uncoupled panel modes and cavity modes contribute to the resonance of the tensioned stiffened double-panel system. We note that, when the cavity is filled with a porous material whose acoustic properties are frequency-dependent, the corresponding eigenequation is non-linear and specific methods are required to calculate the solutions of the resonances equation.

3. PARAMETRIC STUDIES

3.1 Modal properties of the tensioned stiffened double-panel system

The modes and frequencies of a tensioned stiffened skin panel. The first modes and the corresponding natural frequencies of the tensioned and stiffened skin panel, uncoupled from the cavity, are shown in Figure 2. As it will be shown, several of the coupled modes of the double-panel system are dominated by these skin panel resonances. Because we consider a row of identical panels supported by identical stringers for the skin structure, it is observed that the natural frequencies fall in group with the number of natural frequencies within each group equal to the number of panels within a row.

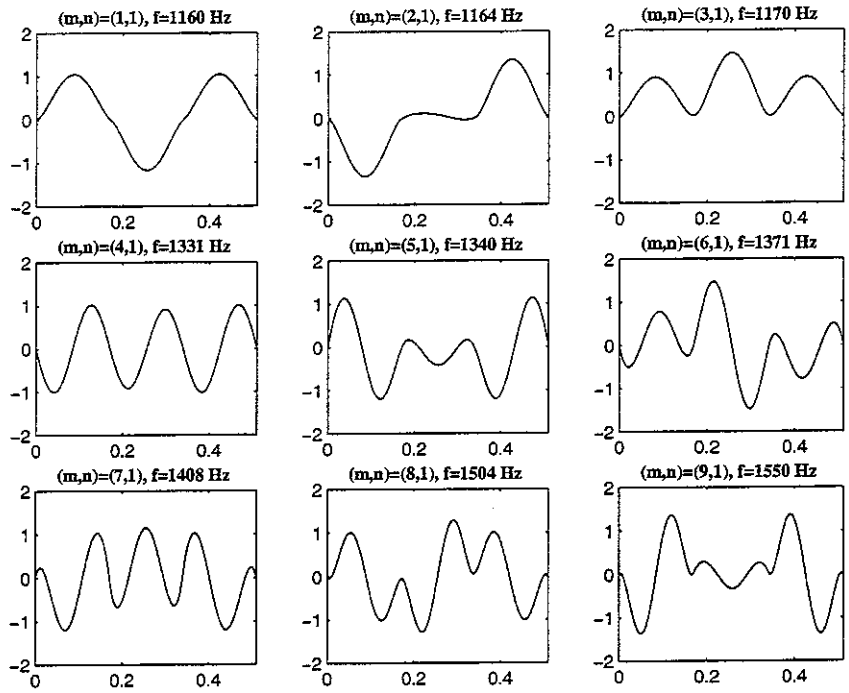

Figure 2. Modes and frequencies of the stiffened and tensioned skin panel.

Resonances of the tensioned stiffened double-panel system. The first resonance modes of the coupled system have been calculated from Eq. (28). Figure 3 shows the mode shapes of the resonances that mostly contribute to the system response, as analysed in the next paragraph, and associated to the tensioned stiffened skin panel and to the trim panel. The two first modes at 210 Hz and 283 Hz correspond to plate-cavity-plate resonances. They represent the effect of the (0,0,0) uniform pressure cavity mode respectively on the (1,1) and on the (1,3) modes of the trim panel. This cavity mode gives rise to equivalent stiffness and subsequently involves a significant increase in the first trim panel resonant frequency (about 36 % for the (1,1) mode) and, to a much lesser extent, in the third resonant frequency (about 2 % for the (1,3) mode). This is due to an important coupling of these modes with the (0,0,0) cavity mode.

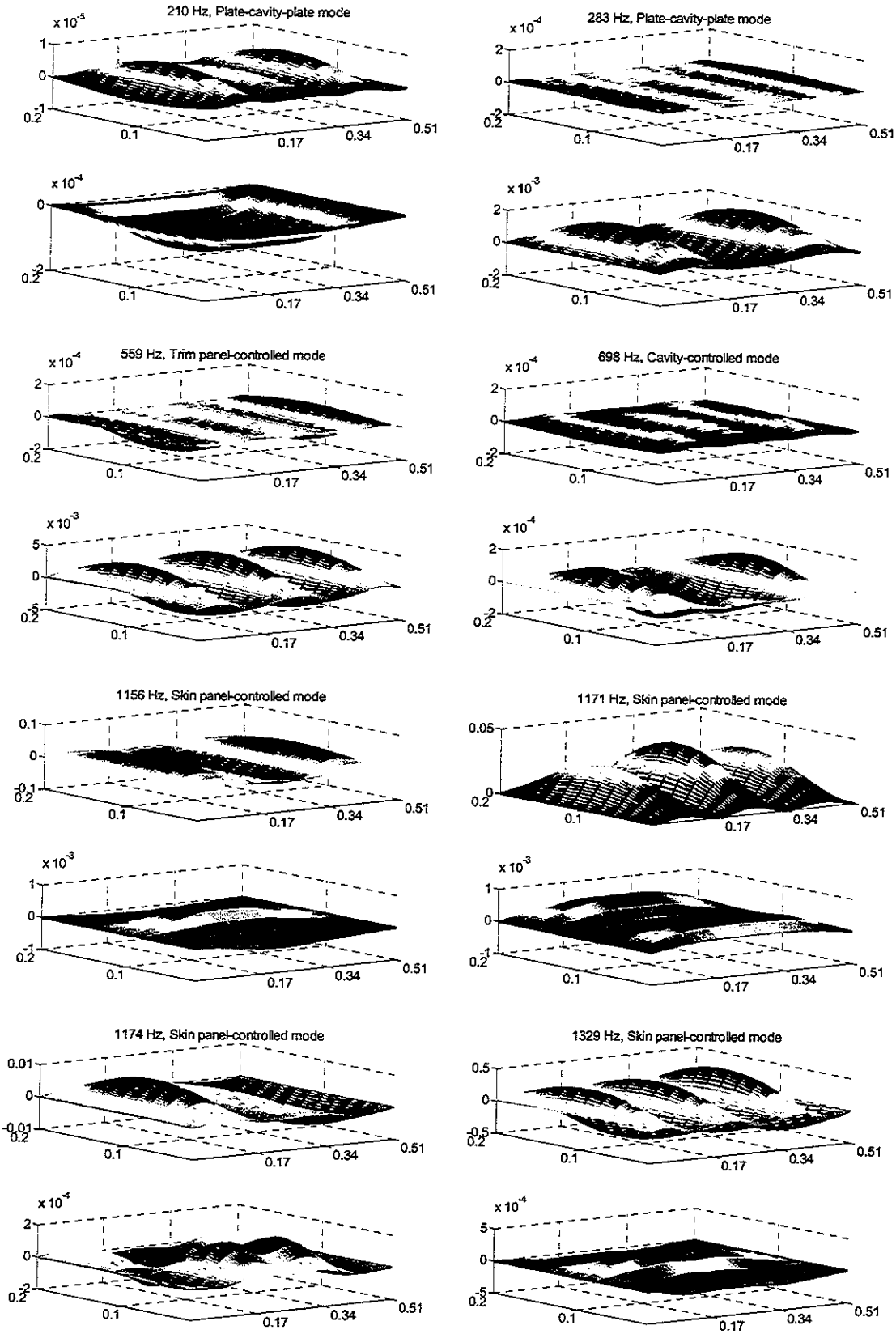

Figure 3. *The mode shapes of the first resonances that mostly contribute to the system response and that are associated to the tensioned stiffened skin panel (top part of each subplot) and to the trim panel (bottom part of each subplot).*

As already noted for the unstiffened double-panel system [57], higher-order plate-cavity-plate resonances can be interpreted as perturbations of structural or cavity resonances. For instance, at 559 Hz, the system response is dominated by a trim panel-controlled mode which is a perturbation of the (1,5) trim panel uncoupled mode with a resonant frequency at 564 Hz. Note that this trim panel resonant frequency is mainly influenced by the closest cavity mode the resonant frequency of which (at 668 Hz) is above the resonant frequency of the trim panel, thus giving rise to equivalent mass. At 698 Hz, we predict a cavity-controlled mode as a perturbation of the (0,2,0) cavity mode that occurs at 668 Hz.

The last four subplots from Figure 3 correspond to tensioned and stiffened skin panel-controlled modes. We note that the skin panel amplitude of these modes is greater than the corresponding trim panel amplitude. The skin panel mode shapes associated to resonances of the coupled system closely follows the uncoupled resonances mode shapes of the tensioned stiffened skin panel shown in Figure 2, apart from the second and third uncoupled resonant frequencies whose respective order has been interchanged due to different coupling strengths with the closest cavity modes that give rise, in this case, to equivalent stiffness. From Figure 3, the local stiffening effect of the stringers can be easily visualised on the succesive modes shapes of the skin panel except for the first resonance mode of the second band (1329 Hz) which corresponds to a "global" mode of the tensioned stiffened skin panel.

3.2 Vibro-acoustic model comparisons for aircraft fuselage panels

Stiffening effect. Figure 4 shows a comparison between the sound power radiated inward by the stiffened double-panel system and by the unstiffened double-panel system, both tensioned and excited by a TBL. The results indicate that, if the effects of stiffeners are neglected, the level of sound power inwardly radiated increases in the low-frequency domain and decreases at higher frequencies. This difference for the stiffened and unstiffened configurations can be interpreted in terms of the hydrodynamic coincidence effect that represents the degree of matching between the TBL wall-pressure fluctuations and the resonant modes.

Figure 5 shows the natural frequencies of the tensioned skin panel, when both stiffened and unstiffened, for different spanwise mode numbers, plotted against the streamwise mode number, along with the hydrodynamic coincidence line for a free-stream velocity of 225 m/s. The proximity of the matching line to the resonant modes determines the importance of highly-excited modes to the response of the aircraft sidewall. It occurs over a frequency range 0-1 kHz for the unstiffened case whereas, for the stiffened case, there are no resonant modes that are coincident below 1 kHz.

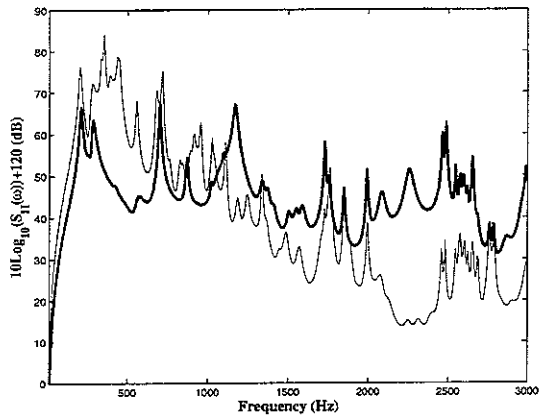

Figure 4. The sound power radiated inward by a tensioned aircraft sidewall excited by a TBL; comparison between the stiffened double-panel model (thick line) and the unstiffened double-panel model (thin line).

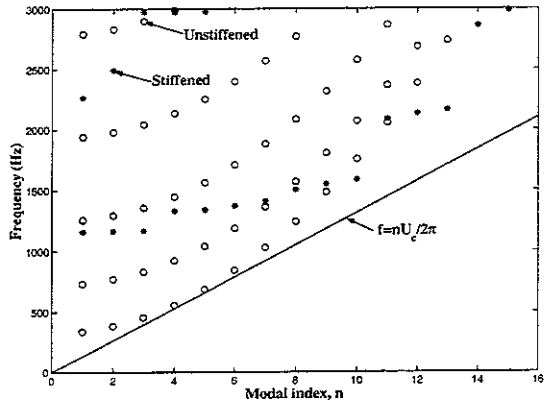

Figure 5. Effect of hydrodynamic coincidence between the modal resonances of the tensioned skin panel, when both stiffened (stars) and unstiffened (circles), for different spanwise mode numbers (m=1, 2 for the stiffened case and m=1,..,5 for the unstiffened case), in terms of the streamwise mode number n, along with the hydrodynamic coincidence line: $\omega/U_c = n\pi/l_{s,y}$ *for a free-stream velocity of 225 m/s.*

Tensioning effect. Figure 6 shows the sound power inwardly radiated by a stiffened double-panel system subject to a TBL excitation, as well as the influence of membrane stresses due to the cabin pressurization, for the parameters given in Table 1. It can be seen that the fundamental frequency of the stiffened skin panel is increased from about 370 Hz to 1160 Hz when tensioning is taken into account. Moreover, unlike in the unstiffened case [5], the mode shapes corresponding to the successive natural frequencies are modified with respect to the unstiffened case (see Eqs. (3-5)). Since the natural frequencies of the stiffened skin panel are lower when in-plane tensions are not accounted for, there is a broader hydrodynamic coincidence range towards the low frequencies. From Figure 6, the contributions from resonant and highly excited modes of the untensioned skin panel are found to dominate the spectrum of the sound power radiated below 1 kHz with respect to the untensioned case. As it has already been noted with other simplified models of aircraft style panels [5, 57], the influence of in-plane tensions cannot be neglected.

Model comparisons. Figure 7 compares the predicted sound power inwardly radiated by the tensioned double-panel system when different models are considered: the stiffened double-panel model, the double-panel model with a single baffled and simply-supported skin panel and the double-panel model with three independent simply supported skin panels. The crosses denote a plate-cavity-plate resonance, the up arrows, a skin panel-controlled resonance, the down arrows, a trim panel-controlled resonance and the circles, a cavity-controlled resonance. In all cases, several plate-cavity-plate resonances are observed below 500 Hz. Above 500 Hz, the resonances are either panel-controlled resonances or cavity-controlled resonances. We also observe that, in this frequency range, the trim-panel controlled modes are so damped that they do not contribute significantly to the sound power radiated for any of the double-panel models.

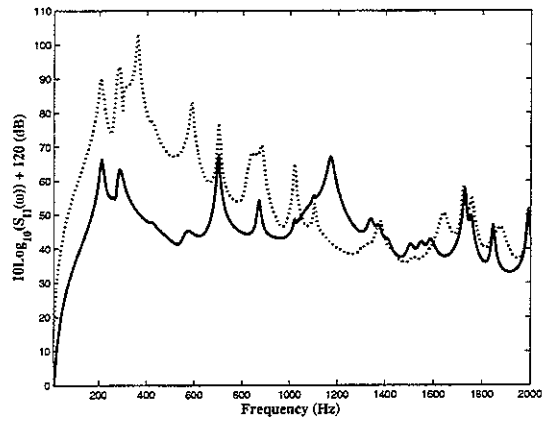

Figure 6. The sound power radiated inward by a stiffened aircraft sidewall excited by a TBL; comparison between the tensioned double-panel model (solid line) and the untensioned double-panel model (dotted line).

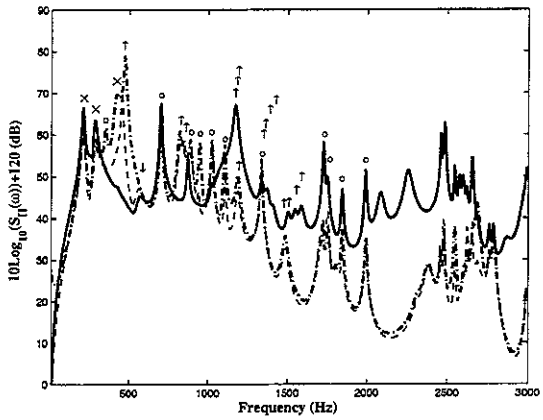

Figure 7. The sound power radiated inward by a tensioned aircraft sidewall excited by a TBL; comparison between the stiffened double-panel model (solid line), the double-panel model with a single baffled skin panel (dashed line) and the double-panel model with three independent simply supported skin panels (dash-dotted line).

First, we note from Figure 7 that the levels of sound power inwardly radiated when the TBL pressure field only excites a single skin panel is slightly lower than the levels obtained when three single skin panels are excited. This is due to a better coupling between the first highly-excited resonances of the skin panel and the cavity for the three panels model with respect to the single panel model, especially at very low-frequencies. Second, above 2 kHz, no coincident and resonant modes are observed for the individual skin panel models whereas, in this frequency range, a large number of resonant modes are already highly-excited for the stiffened skin panel model and these modes occur within frequency bands. This explains the significant differences observed in the sound power radiated above 2 kHz between the stiffened configuration and the unstiffened configuration. Below 2 kHz, the spectrum levels are quite similar in both cases except in the vicinity of the first highly excited resonance of the simply-supported skin panel where differences of about 30 dB are observed.

Cavity damping effect. The sound power inwardly radiated by the tensioned and TBL-excited double-panel system with air between the panels is plotted in Figure 8. It can be compared with the sound power radiated when fiberglass is inserted within the cavity. In this configuration, we observe that the cavity-controlled modes are so damped that the resonant response of the cavity is not seen in the spectrum of the sound power radiated. As a

consequence, it is the stiffened skin panel-controlled modes that mainly govern the vibro-acoustic response of the panel-fiberglass-panel system. It can also be seen that the insertion of fiberglass between the panels has a beneficial effect on the radiated power at most frequencies except in the vicinity of some bands of skin panel-controlled modes that are excited with enough efficiency to overcome the added damping due to the cavity treatment. However, because the overall sound power radiated is mainly determined by the contribution of the first few skin panel-controlled modes, the magnitude of which is weakly modified by the insertion of the fiberglass treatment, only 5 dB reduction is observed in the total sound power radiated up to 3 kHz when the fiberglass is inserted into the cavity instead of air. Thus, the passive treatment really starts to be efficient on the overall levels only above the first few stiffened skin panel-controlled modes, i.e. above 1.5 kHz in our configuration. It is therefore of interest to investigate the performance of different active control strategies in order to compensate for the limited noise reduction obtained by passive treatments in the low-frequency domain.

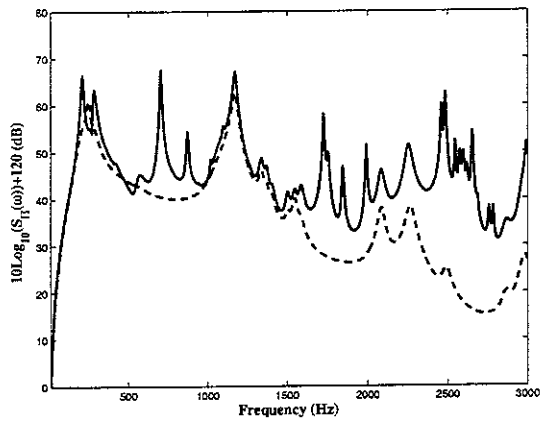

Figure 8. *The sound power radiated inward by a tensioned aircraft sidewall excited by a TBL; comparison between the stiffened double-panel with air cavity (solid line) and the stiffened double-panel with fiberglass cavity (dashed line).*

4. PHYSICAL LIMITATION OF ACTIVE CONTROL PERFORMANCE

In order to assess the performance of active structural acoustic control (ASAC) and cavity control, comparisons are presented of the noise reduction obtained by actively controlling the structural modes of either the stiffened skin panel or the trim panel and the acoustic modes of the cavity. Physically, this can be interpreted as a feedback control system using collocated actuator/sensor pairs which could achieve perfect cancellation of each kind of mode while ensuring unconditional stability whatever the magnitude of the feedback gain [5]. Figures 9, 10 and 11 show the effect of canceling the first modes of the following subsystems: the stiffened skin panel structural modes, the trim panel structural modes and the cavity modes. The corresponding attenuations in terms of the total sound power radiated up to 1 kHz and 3 kHz are summarized in Table 2.

Panels structural modes control. From Figure 9, it can be seen that suppressing the two first structural modes of the skin panel has a negligible effect on the reduction of the sound power radiated whereas suppressing higher order modes of the skin panel will cause a significant attenuation (about 21 dB with 3 control channels). First, this is due to the fact that, when they are resonant, the two first skin panel modes are less efficiently excited by the TBL pressure fluctuations than the higher order modes, as it can be observed from Figure 5. The second point is that, at their excitation frequencies (about 1160 Hz), the two first skin panel modes do not couple well with the nearest cavity mode (the (1,2,0) mode which becomes resonant at 1083 Hz) whereas there is a strong degree of coupling between this cavity mode and the third skin panel mode. It is a combination of these effects that explains why significant reductions in the sound power radiated are only achieved after cancellation of the third skin panel structural mode. In the light of the discussion related to Figure 5, we also understand that suppressing the contribution of higher order skin panel modes, that are highly-excited when they are resonant, will cause a significant reduction for the total sound power radiated, as it can be observed from Table 2.

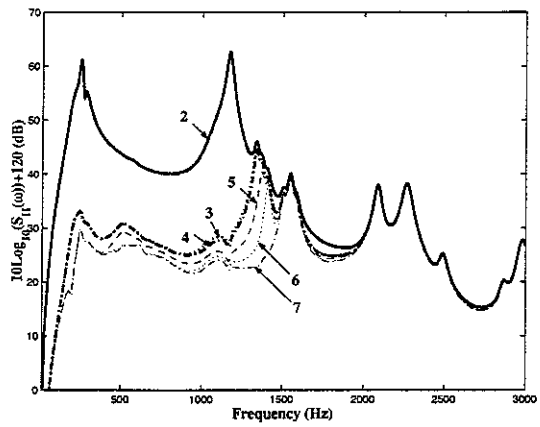

Figure 9. The sound power radiated inward by an aircraft sidewall excited by a TBL when controlling the structural modes of the stiffened skin panel; thick solid line: before control and after cancellation of the two first structural modes of the skin panel; dotted line: after cancellation of its three first structural modes; dashed line: after cancellation of its four first structural modes; thin dashed line: after cancellation of its five first structural modes; thin dotted line: after cancellation of its six first structural modes; thin dash-dotted line: after cancellation of its seven first structural modes.

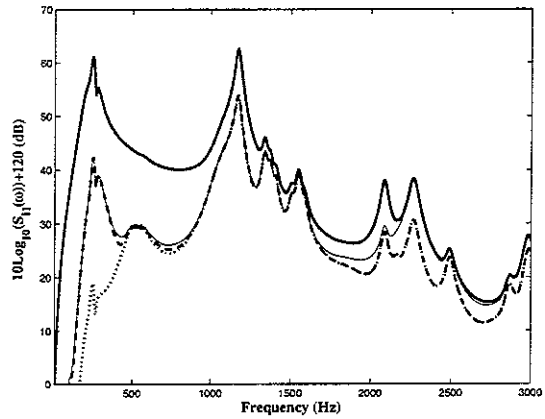

Figure 10. The sound power radiated inward by an aircraft sidewall excited by a TBL when controlling the structural modes of the trim panel; thick solid line: before control; faint solid line: after cancellation of the first structural mode of the trim panel; dashed line: after cancellation of its two first structural modes; dotted line: after cancellation of its three first structural modes.

From Table 2, it can also be seen that approximately the same level of attenuation for the total sound power radiated in the low frequency domain can be achieved by canceling the contribution of at least the three first structural modes of the skin panel or the trim panel (about 21 dB for the sound power radiated up to 1 kHz). However, as already observed for the unstiffened model [57], reductions in the total sound power radiated up to 3 kHz are achieved more efficiently when suppressing the contributions of the skin panel modes compared with the trim panel modes. Indeed, over a broad frequency range, the skin panel-controlled modes govern the resonances that mostly contribute to the vibro-acoustic response of the double-panel system whereas the trim panel-controlled modes are so damped that their suppression is only effective in the very low-frequency domain.

	Attenuation up to 3 kHz						**Attenuation up to 1 kHz**					
Number of modes controlled	**1**	**2**	**3**	**4**	**5**	**6**	**1**	**2**	**3**	**4**	**5**	**6**
Skin panel modes	0.1	0.3	15.8	16	17.8	18.8	0.2	0.4	21	21.2	23.5	24.5
Cavity modes	4.3	4.4	5	5.1	5.1	5.2	14.4	14.5	17	17.4	17.4	17.5
Trim panel modes	9.7	9.9	10.2	10.3	10.7	10.8	17.2	17.5	21.9	22	23.7	23.8

***Table 2.** Attenuation in the total sound power radiated by the stiffened double-panel system calculated up to 3 kHz and up to 1 kHz after cancellation of the first structural modes of the skin panel, after cancellation of the first cavity modes and after cancellation of the first structural modes of the trim panel.*

An interesting feature observed in Figure 10 concerns the fact that suppressing the very first structural modes of the trim panel has a beneficial effect on the higher order trim panel resonances. This is because first, they are mutually coupled with the actively controlled modes through the shallow cavity and second, because they have resonance frequencies very close to the highly-excited resonances of the skin panel modes. For instance, we note that the cancellation of the first trim panel mode, that is resonant at 134 Hz, will cause a significant reduction in the contribution to the sound power radiated of the (3,3) mode and the (3,7) mode of the trim panel that couple well with the (1,1) mode and that are respectively resonant at 1209 Hz and 2100 Hz, i.e within

frequency ranges where skin panel resonances dominate the spectrum levels of sound power radiated.

Cavity modes control. From Figure 11, it can be seen that the suppression of cavity modes with a limited number of control channels is only efficient in the very low frequency domain, as observed by Bao *et al.* [41] for tonal excitation and Maury *et al.* [57] for TBL excitation of an unstiffened double-panel. As observed from Table 2, the active control of cavity modes is the less efficient strategy in terms of reduction of the total sound power radiated up to 3 kHz, but significant attenuations are observed in the very low frequency domain, i.e. when we consider the total sound power radiated up to 1 kHz. They are almost comparable to those obtained by actively controlling the trim panel modes (only 3 dB differences with 2 control channels).

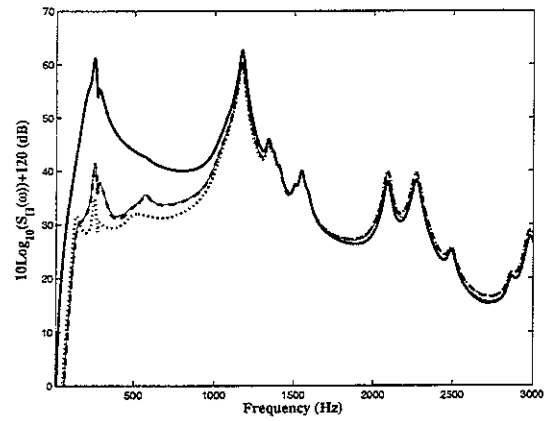

Figure 11. *The sound power radiated inward by an aircraft sidewall excited by a TBL when controlling the cavity modes; thick solid line: before control; faint solid line: after cancellation of the first cavity mode; dashed line: after cancellation of its two first cavity modes; dotted line: after cancellation of its three first cavity modes.*

5. CONCLUSIONS

In view of the results presented in this paper, it appears that the prediction of the sound power inwardly radiated by a stiffened double-partition excited by a TBL should account for the dynamics of discretely stiffened skin panels since significant differences can be observed if the elastic stringers are replaced by simple-support boundary conditions. However, accounting for the stiffening effect of stringers on the skin panel does not modify drastically the conclusions previously reached [57] concerning the performance of active feedback control of the boundary layer induced noise for the double-panel model with rigid reinforcements: it is the strategy based on the active suppression of the skin panel structural modes that is the most efficient in terms of the broadband attenuation of the total sound power inwardly radiated. However, it has been shown that in the low frequency domain, the inwardly radiated sound power can still be reduced by about 17 dB if only the first trim panel mode is actively controlled, or by about 14 dB if the first acoustic mode of the cavity is actively controlled.

6. ACKNOWLEDGEMENTS

The first author of this study has been sponsored by the Engineering and Physical Sciences Research Council under the Grant No. N21529/01.

7. REFERENCES

[1] J. S. MIXSON and J. F. WILBY (1995) "Interior Noise" in *Aeroacoustics of Flight Vehicles, Theory and Practice*, edited by H. H. Hubbard, NASA Langley Research Center, Hampton, VA. Chap. 16, pp. 271-355.

[2] P. GARDONIO (2002) *Journal of Aircraft* **39** (2), 206-214. Review of active techniques for aerospace vibro-acoustic control.

[3] W. V. BHAT (1971) *Journal of Sound and Vibration* **14** (4), 439-457. Flight test measurement of exterior turbulent boundary layer pressure fluctuations on Boeing model 737 airplane.

[4] J. F. WILBY and F. L. GLOYNA (1972) *Journal of Sound and Vibration* **23** (4), 443-466. Vibration measurements of an airplane fuselage structure. Part I: turbulent boundary excitation.

[5] C. MAURY, P. GARDONIO and S. J. ELLIOTT (2001) *American Institute of Aeronautics and Astronautics Journal* **39** (11), 1860-1867. Active control of the flow-induced noise transmitted through a panel.

[6] C. MAURY, P. GARDONIO and S. J. ELLIOTT (2002) *Journal of Sound and Vibration* **252** (1), 83-113. A wavenumber approach to modelling the response of a randomly excited panel, part I: general theory.

[7] C. MAURY, P. GARDONIO and S. J. ELLIOTT (2002) *Journal of Sound and Vibration* **252** (1), 115-139. A wavenumber approach to modelling the response of a randomly excited panel, part II: application to aircraft panels excited by a turbulent boundary layer.

[8] C. MAURY, P. GARDONIO and S. J. ELLIOTT (2002) *American Institute of Aeronautics and Astronautics Journal* **40** (6), 1113-1121. Modelling study for the active control of the flow-induced noise transmitted through a double-panel system.

[9] M. J. CROCKER (1969) *Journal of Sound and Vibration* **9** (1), 6-20. The response of a supersonic transport fuselage to boundary layer and to reverberant noise.

[10] C. MAURY, P. GARDONIO and S. J. ELLIOTT (2001) *Proceedings of the 17thInternational Congress on Acoustics,* in Vol. I, section *Vibrations and structural acoustics.* A wavenumber approach for the response of aircraft sidewalls to random pressure fluctuations.

[11] H. G. DAVIES (1971) *Journal of the Acoustical Society of America* **55**, 213-219. Sound from turbulent boundary layer excited panels.

[12] L. MAESTRELLO (1967) *Journal of Sound and Vibration* **5** (3), 407-448. Use of turbulent models to calculate the vibration and radiation responses of a panel, with practical suggestions for reducing sound levels.

[13] G. ROBERT (1984) *Ph. D. Thesis No. 84-02, Ecole Centrale de Lyon, France.* Modelisation et simulation du champ excitateur induit sur une structure par une couche limite turbulente.

[14] P. J. T. FILIPPI and D. MAZZONI (1994) In *Boundary Elements XVI* (C. A. Brebbia, editor), 47-54, Southampton-Boston: Computational Mechanics Publications. Noise induced inside a cavity by an external turbulent boundary layer.

[15] W. R. GRAHAM (1996) *Journal of Sound and Vibration* **192** (1), 101-120. Boundary layer induced noise in aircraft, part I: the flat plate model.

[16] W. R. GRAHAM (1997) *Journal of Sound and Vibration* **206** (4), 541-565. A comparison of models for the wavenumber-frequency spectrum of turbulent boundary layer pressures.

[17] Y. F. HWANG and G. MAIDANIK (1990) *Journal of Sound and Vibration* **142** (1), 135-152. A wavenumber analysis of the coupling of a structural mode and flow turbulence.

[18] K. H. HERON (1978) *Ph.D. Thesis, Institute of Sound and Vibration Research, University of Southampton,* Boundary-layer-induced cabin noise.

[19] S. F. WU. G. WU, M. M. PUSKARZ, and M. E. GLEASON (1997) *Journal of Vibration and Acoustics* **119** (4), 557-562. Noise transmission through a vehicle side window due to turbulent boundary layer excitation.

[20] F. HAN, R. J. BERNHARD and L. G. MONGEAU (1999) *Journal of Sound and Vibration* **227** (4), 685-709. Prediction of flow-induced structural vibration and sound radiation using energy flow analysis.

[21] D. C. TOMLINSON (2001) *Progress Report 2.2.6a,* In *Project ENABLE (Environmental Noise Associated with Turbulent Boundary Layer Excitation), EU Research Programme FP5 Contract No. GR4D-CT-2000-00223.* SEA theory for TBL-induced noise and vibration.

[22] S. BRUHL and J. REICHENBERGER (2001) *Progress Report 2.1.6a,* In *Project ENABLE (Environmental Noise Associated with Turbulent Boundary Layer Excitation), EU Research Programme FP5 Contract No. GR4D-CT-2000-00223.* Basic AutoSEA2 Modelisation of Boeing Flight Tests.

[23] D. J. MEAD and K. K. PUJARA (1971) *Journal of Sound and Vibration* **14** (4), 525-541. Space-harmonic analysis of periodically supported beams: response to convected random loading.

[24] D. J. MEAD and A. K. MALLIK (1976) *Journal of Sound and Vibration* **47** (4), 457-471. An approximate method of predicting the response of periodically supported beams subjected to random convected loading.

[25] F. BIRGERSSON, N. S. FERGUSSON and S. FINNVEDEN *Journal of Sound and Vibration (In Press).* Application of the Spectral Finite Element Method to Turbulent Boundary Layer Induced Vibration of Plates.

[26] R. A. MKHITAROV (1975) *Soviet Physics Acoustics* **20** (6), 528-533. Sound radiation from a bounded thin inhomogeneous plate reinforced with N ribs and driven by boundary-layer pressure fluctuations.

[27] Y. K. LIN and B. K. DONALDSON (1969) *Journal of Sound and Vibration* **10** (1), 103-143. A brief survey of transfer matrix techniques with special reference to the analysis of aircraft panels.

[28] F. LECKIE and E. PESTEL (1960) *International Journal of Mechanical Science* **2**, 137-167. Transfer-matrix fundamentals.

[29] R. VAICATIS and M. SLAZAK (1980) *Journal of Sound and Vibration* **70** (3), 413-426. Noise transmission through stiffened panels.

[30] C. S. LYRINTZIS and D. A. BOFILIOS (1990) *Journal of Aircraft* **27** (8), 722-730. Hygrothermal Effects on structure-borne noise transmission of stiffened laminated composite plates.

[31] C. S. LYRINTZIS and R. VAICATIS (1990) *Journal of Aircraft* **27** (2), 176-184. Random response and noise transmission of discretely stiffened composite panels.

[32] M. T. CHANG and R. VAICATIS (1982) *Journal of Sound and Vibration* **85** (1), 71-83. Noise transmission into semicylindrical enclosures through discretely stiffened curved panels.

[33] M. L. RUMERMAN (2001) *Journal of the Acoustical Society of America* **109** (2), 563-575. Estimation of broadband acoustic power due to rib forces under turbulent boundary layer-like excitation. I. Derivation using string model.

[34] M. L. RUMERMAN (2001) *Journal of the Acoustical Society of America* **109** (2), 576-582. Estimation of broadband acoustic power due to rib forces under turbulent boundary layer-like excitation. II. Applicability and validation.

[35] M. L. RUMERMAN (2002) *Journal of the Acoustical Society of America* **111** (3), 1274-1279. Estimation of broadband acoustic power radiated from a turbulent boundary layer-driven reinforced finite plate section due to rib and boundary forces.

[36] Y. M. HUANG and C. R. FULLER (1998) *Journal of Vibration and Acoustics* **120** (2), 496-502. Vibration and Noise Control of the Fuselage via Dynamic Absorbers.

[37] U. EMBORG, S. LETH, F. SAMUELSON and J. HOLMGREN (1998) *Proceedings of the 4th AIAA/CEAS Aeroacoustics Conference*, Paper No. 98-2231. Active and Passive Noise Control in Practice on the SAAB 2000 High Speed Turboprop.

[38] J. SILCOX, K, H. LYLE, V. L. METCALF and D. E. BROWN (1995) *Proceedings of the 1st AIAA/CEAS Aeroacoustics Conference*, Paper No. 95-161. A Study of Active Structural Acoustic Control Applied to the Trim Panels of a Large Scale Fuselage Model.

[39] A. von FLOTOW, M. MERCADAL and M. TAPPERT (2000) *U. S. Patent 6,078,673.* Apparatus and Method for Active Control of Sound Transmission Through Aircraft Fuselage Walls.

[40] J. PAN and C. BAO (1998) *Journal of the Acoustical Society of America* **103** (4), 1916-1922. Analytical study of different approaches for active control of sound transmission through double walls.

[41] C. BAO and J. PAN (1997) *Journal of the Acoustical Society of America* **102** (3), 1664-1670. Experimental study of different approaches for active control of sound transmission through double walls.

[42] S. J. ELLIOTT, C. C. BAUCHER and P. A. NELSON (1992) *IEEE Transactions on Signal Processing* **40** (5), 1041-1052. The Behaviour of a Multiple Channel Active Control System.

[43] S. J. ELLIOTT, P. GARDONIO, T. J. SORS and M. J. BRENNAN (2002) *Journal of the Acoustical Society of America* **111** (2), 908-915. Active Vibro-Acoustic Control with Multiple Local Feedback Loops.

[44] C. R. FULLER (2002) *Proceedings of ACTIVE 2002*, in *Distinguished Lectures*. Active control of sound radiation from structures: progress and future directions.

[45] G. P. GIBBS and R. H. CABELL (2002) *Proceedings of the 8th AIAA/CEAS Aeroacoustics Conference*, Paper No. 2002-2496. Active control of turbulent boundary layer induced sound radiation from multiple aircraft panels.

[46] J. S. BEVAN (1998) *NASA-CR-1998-207667*. Analysis and testing of plates with piezoelectric sensors and actuators.

[47] C. R. FULLER , M. E. JOHNSON and J. R. GRIFFIN (2000) *Proceedings of the 6th AIAA/CEAS Aeroacoustics Conference*, Paper No. 2000-2041. Active-passive control of aircraft interior boundary layer noise using smart foams.

[48] C. R. FULLER (2000) *Proceedings of the 8th Conference on Nonlinear Vibrations, Stability and Dynamics of Structures*. Control of large distributed structures with numerous actuators and biologically inspired control architecture.

[49] D. R. THOMAS and P. A. NELSON (1995) *Journal of the Acoustical Society of America* **98** (5), 2651-2662. Feedback control of sound radiation from a plate excited by a turbulent boundary layer.

[50] E. FRIOT, M. GEORGELIN, ROBERT G. and DURAND C. (1999) *Proceedings of Forum Acusticum 1999*. Real-time control of a vibrating plate excited by a turbulent boundary layer.

[51] C. M. HEATWHOLE, M. A. FRANCHEK and R. J. BERNHARD (1997) *Journal of the Acoustical Society of America* **102** (2), 989-997. Robust feedback control of flow-induced structural radiation of sound.

[52] G. P. GIBBS, R. CABELL and J. JUANG (2000) *Proceedings of the 6th AIAA/CEAS Aeroacoustics Conference*, Paper No. 2000-2043. Controller complexity for active control of TBL induced sound radiation from panels.

[53] P. AUGEREAU (2001) *ISVR Technical Memorandum* **869**. Feedback control of the sound inwardly radiated by an aircraft panel excited by a turbulent boundary layer.

[54] W. R. GRAHAM (1996) *Journal of Sound and Vibration* **192** (1), 121-138. Boundary layer induced noise in aircraft, part II: the trimmed flat plate model.

[55] D. A. BIES (1971) *Noise and Vibration Control*, chapter **10**. Acoustical properties of porous materials. L.L. Beranek editor, New-York: McGraw-Hill Book Company.

[56] G. M. CORCOS (1967) *Journal of Sound and Vibration* **6** (1), 59-70. The resolution of turbulent pressure at the wall of a boundary layer.

[57] C. MAURY, P. GARDONIO and S. J. ELLIOTT (2002) *American Institute of Aeronautics and Astronautics Journal* **40** (6), 1860-1867. Model for active control of flow-induced noise transmitted through double partitions.

Appendix A

Transformation and reduction of the integral (25)

We now derive an analytical expression for the generic integral (25) that appears in the calculation of the modal excitation terms given in Section 2 by Eq. (15). The integral (25) takes the form:

$$I(\alpha,\beta)=\int_0^a\int_0^a e^{i(\alpha y+\beta y')}e^{-K_y|y-y'|}e^{ik_c(y-y')}dydy' \tag{A.1}$$

where α and β denote complex numbers. We now consider the following transformation for the integration variables that appear in integral (A.1):

$$\begin{cases}\xi = y-y' \\ \chi = y\end{cases} \tag{A.2}$$

so that the original integration contour is deformed as illustrated in Figure A.1.

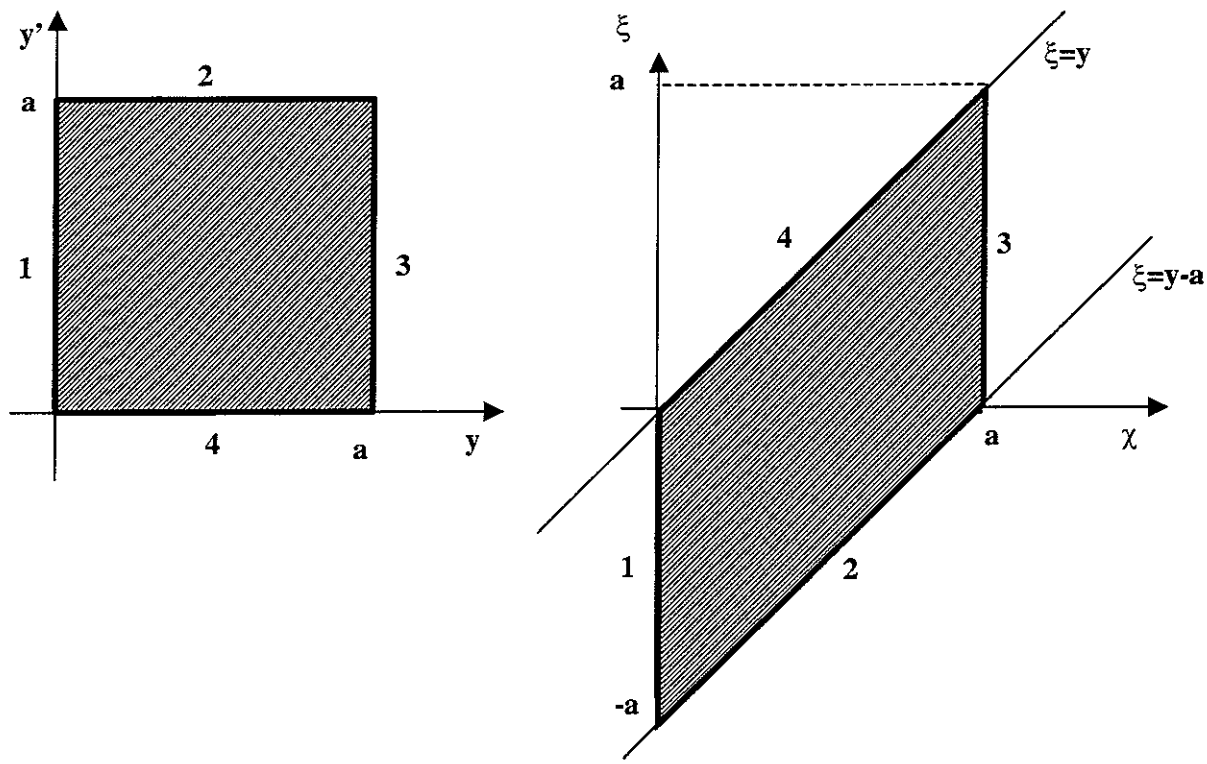

Figure A.1. Transformation of the integration contour.

Under the transformation (A.2), integral (A.1) reads:

$$I(\alpha,\beta)=-\int_y^{y-a}\int_0^a e^{i(\alpha+\beta)\chi}e^{-K_y|\xi|}e^{i(k_c-\beta)\xi}d\chi d\xi \tag{A.3}$$

The ξ - and χ -integrations are interchanged and the integration is performed over the dashed area (Figure A.1). Therefore:

$$I(\alpha,\beta)=\left(\int_{-a}^{0}\int_{0}^{\xi+a}+\int_{0}^{a}\int_{\xi}^{a}\right)e^{i(\alpha+\beta)\chi}e^{-K_y|\xi|}e^{i(k_c-\beta)\xi}d\chi d\xi \tag{A.4}$$

Two cases have to be considered for the χ -integration:

If $\alpha+\beta\neq 0$:

$$I(\alpha,\beta)=\frac{1}{i(\alpha+\beta)}\int_{0}^{a}e^{-K_y\xi}\left(e^{i(\alpha+\beta)(a-\xi)}-1\right)\left(e^{i(\alpha+k_c)\xi}+e^{i(\beta-k_c)\xi}\right)d\xi \tag{A.5}$$

If $\alpha+\beta=0$:

$$I(\alpha,\beta)=2\int_{0}^{a}e^{-K_y\xi}(a-\xi)\cos\left((\beta-k_c)\xi\right)d\xi \tag{A.6}$$

Analytical evaluation of these integrals can be performed either using direct integration or integration by parts giving:

If $\alpha+\beta\neq 0$:

$$\begin{aligned}I(\alpha,\beta)=\frac{1}{i(\alpha+\beta)}\Big\{e^{i(\alpha+\beta)}\Big[&F\left(-i(\beta-k_c)-K_y\right)+F\left(-i(\beta+k_c)-K_y\right)\Big]\\&-\Big[F\left(i(\alpha+k_c)-K_y\right)+F\left(i(\alpha-k_c)-K_y\right)\Big]\Big\},\end{aligned} \tag{A.7}$$

If $\alpha+\beta=0$:

$$I(\alpha,\beta)=\frac{2aK_y}{K_y^2+(k_c-\beta)^2}+2\Re\left[\frac{F\left(-i(\beta-k_c)-K_y\right)}{-i(\beta-k_c)-K_y}\right], \tag{A.8}$$

where: $F(z)=\dfrac{e^z-1}{z}$. The corresponding analytical continuations of (A.7) and (A.8) are readily obtained when z tends towards zero.